Fatima M. Ahmed[1,2]
Mohammed K. Jawad[1]

[1] *Department of Physics, College of Science, University of Baghdad, Baghdad, IRAQ*
[2] *Department of Physics, College of Science, Al-Nahrain University, Jadriya, Baghdad, IRAQ*

Characterization of Blend Electrolytes Containing Organic and Inorganic Nanoparticles

Gels of PVA/PVP polymer nanocomposite electrolytes filled with gradient contents of SiO_2 and MWCNT were fabricated using a solution casting technique. The interaction of the polymer nanocomposite electrolytes was confirmed by FTIR investigation. The Electrical conductivity was calculated with an impedance analyzer within the frequency range 50 Hz–1 MHz at a temperature range 293–343 K has the highest ionic conductivity with 10 wt. % of MWCNTs and 6 wt.% of SiO_2. The real dielectric constant was higher at lower frequencies. Faster-conducting electrolyte ions appeared to require less energy to move, according to the reduction in activation energy. Differential scanning calomatric thermograms showed a single glass transition temperature that confirms the miscibility of PVA and PVP together with the nanoparticles.

Keywords: Blend electrolytes; Dielectrics; Bulk resistance; Thermal analysis
Received: 28 August 2023; **Revised:** 02 October 2023; **Accepted:** 09 October 2023

1. Introduction

Nanomaterials were studied in various fields such as physics, chemistry, materials sciences, medicine, biology and pharmacy, due to their unique electronic and optical properties. The characteristics of particles are enhanced by decreasing their size. The chemical and physical characteristics of nanomaterials play a crucial role in determining their suitability for various applications [1].

Nanomaterials have a significant influence on ionic conductivity, especially when incorporated with materials designed for using in energy storage devices, sensors, fuel cells and other electrochemical applications. Nanomaterials can be incorporated into the design of solid or gel electrolyte nanocomposites to improve their ionic conductivity. For instance, nanoparticles or nanofibers can be added to polymer electrolytes to enhance their ion transport properties. However, the effect of nanomaterials on ionic conductivity is complex and based on various factors such as type of nanoparticles and electrolyte [2-4].

Nanocomposite materials that are created by combining two or more distinct construction components into a single material that have unique properties due to their small size, large surface area and the interfacial interaction between phases. Nanocomposite based on the concept of using building elements with nanometer-scale dimensions to develop and construct new materials with unprecedented flexibility and improvement of their physical properties [5].

Poly vinyl alcohol (PVA) is a synthetic hydrophilic linear polymer that is highly soluble in water due to its large number of hydroxyl groups, which interact with water molecules through hydrogen bonds [3]. PVA is highly flexible, transparent and biocompatible, making it an indispensable material in the microelectronics, textile, paper, adhesives, food, biomedical and pharmaceutical industries. The high hydrophilicity and processability of PVA enable its compatibility with many different kinds of synthetic and natural polymer [7, 8].

Poly vinylpyrolidone (PVP) is a water-soluble macromolecular compound that is readily soluble in water and most polar organic solvents. It exhibits exceptionally low toxicity and high biocompatibility, making it useful as a medication carrier in pharmaceutical technology [9]. PVA and PVP are examples of biodegradable polymers that exhibit solubility in water because of the robust hydrogen bonding interactions formed between the functional groups in the polymers and water molecule [10, 11].

Silica (SiO_2) nanoparticles are frequently employed as nanofillers in thermoplastics and thermosetting polymers due to the exceptional characteristics of PVA and PVP, such as ease of synthesis, thermal stability, high specific surface area, durability and mechanical strength. Despite the known carcinogen crystalline silica, these nanoparticles are completely amorphous, non-toxic, and non-irritating [12].

Multi-walled carbon nanotubes (MWCNTs) consist of multiple layers of single-walled carbon nanotubes, which are narrow strips of graphene rolled into seamless tubes. These tubes are engineered in a

concentric manner with their diameter progressively increasing. Carbon nanotubes (CNTs) possess distinctive electronic and mechanical characteristics that make them highly suitable for various industrial applications. Nevertheless, owing to the presence of Vander Waals forces, carbon nanotubes tend to clump together, forming aggregates. This tendency poses a significant challenge when it comes to dispersing and aligning them within a polymer matrix [13].

2. Experimental Part

The used material in this project are PVA (MW ~14000), PVP (MW ~40000), DMSO, EC, PC, KI, I_2, SiO_2, MWCNT with high purity of more than 98%.

The samples were fabricated using a fixed proportion of PVP, PVA (50:50), PC, EC (1:1), 50 wt.% KI and iodine I_2 = 10% of salt wt.%, along with varying proportions of Nano SiO_2 and MWCNTs. First, sufficient amounts of EC, PC, and PVA were mixed together in a glass tube for 2 hours at 30°C with continuous stirring. Then, PVP and KI were added to the mixture and stirrer for 2 hours. Followed by adding the nanoparticles to the mixture to get two groups of electrolytes labeled as B and C. These electrolytes contain nanoparticles of SiO_2 and MWCNTs with various percentages, as shown in table (1). To prevent agglomeration and aggregation, the nanoparticles were added slowly to the electrolytes with continuous stirring for 1 to 3 hours. Finally, iodine (I_2) was added to the mixture while stirring continuously at room temperature for 30 minutes until gelation occurs.

Table (1) Composition of gel electrolytes system B and C

Electrolytes Type	Nanoparticles wt.%				
	2	4	6	8	10
PVA-PVP-KI-SiO_2	B1	B2	B3	B4	B5
PVA-PVP-KI-MWCNTs	C1	C2	C3	C4	C5

FTIR spectra were collected at temperature using a Perkin Elmer Spectrum instrument, covering a wavelength range of 400-4000 cm^{-1}. The electrical conductivity of the samples was determined using an LCR-811G/815G impedance analyzer, which operated within the frequency range of 50 Hz to 1 MHz. The ionic conductivity (σ) of each sample was calculated using the following equation [14]:

$$\sigma = L/(R_b \times A) \quad (1)$$

where L(cm) represents the distance between the electrodes, R_b is the bulk resistance and A (cm^2) is the electrode area. The temperature of the sample was changed from the range of 293 K to 343 K. The values of the real parts of the dielectric constant (ε_r) were determined using the following equation [15]:

$$\varepsilon_r = z_i / (\omega C_0 \times (z_r^2 + z_i^2)) \quad (2)$$

In this equation,"r presents the angular frequency=$2\pi f$ [16] , C_0 is the vacuum-capacitance, and z_r and z_i are the real and imaginary parts of the resistance, respectively. The DSC measurements of the samples were performed using SDT Q600 V20.9 Build 20 system. The DSC thermographs were recorded within the temperature range of 0 to 1000 °C under the argon atmosphere.

3. Results and Discussion

Figure (1) illustrates FTIR spectrum of the SiO_2 nanocomposites which is related to the band at 3414.78-3441.75 cm^{-1} to the Si-OH stretching of silanol bonded (Si) to a hydroxyl group (–OH) [14]. The peaks that positioned at 2990.59, 2926.75 and 2825.22 cm^{-1} are corresponded to asymmetric stretching vibration and symmetric stretching of C-H, respectively [18-20]. The bands at (1800.88-1665.25) and (143.25-1439.25) cm^{-1} were assigned to -C=O stretching vibration and -C=N pyridine ring stretching, respectively. The twisting of the CH_2 group is lower than from 1289.96 to 1179.25 cm^{-1} [18, 21] as shown in Fig. (1) (B1-B2) and table (2).

The nanocomposite samples showed overlapping bands in the region of 1036.67 cm^{-1} to 703.69 cm^{-1}, which corresponded to the SiO_2 nanoparticles and the (PVP-PVA) blend. Specifically, observed the asymmetric stretching vibration of the Si-O-Si at (953.85 cm^{-1}) and symmetric stretching vibration of the Si-O-Si at (703.69 cm^{-1}) groups were observed [22].

The nanocomposites consist of functional groups derived from both the SiO_2 nanoparticles and the polymers. The miscibility of polymer electrolytes is confirmed by the presence of hydrogen bonding between the carbonyl C=O and hydroxyl -OH functional groups (H–O …… C=O), as indicated by observed relative changes in intensities and positions" [23].

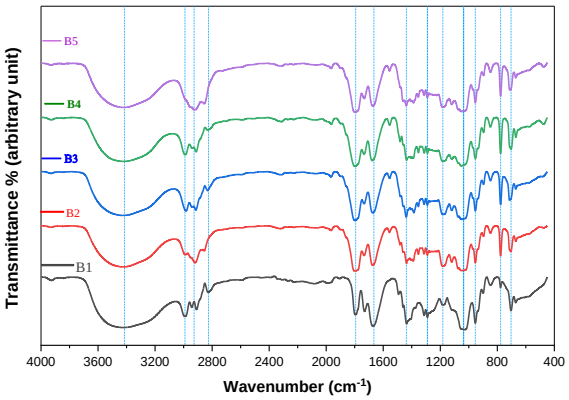

Fig. (1) FTIR spectra of blend nanocomposites with various weight percentages of SiO_2

The spectra of (PVA/PVP/KI) polymer blends filled with various MWCNTs (2, 4, 6, 8, and 10 wt. %) are displayed in Fig. (2). The peak which corresponded to the stretching of (OH) at 3426.5 cm^{-1} displayed variation and shifted towards a lower wavenumber with an increase in the MWCNTs content, as demonstrated in table (3). The band which is associated with the asymmetric stretching vibration of CH_2 was observed around 2925.5 cm^{-1}. The peak at approximately 1794.5 cm^{-1} was attributed to the

stretching mode of C=C. The intensity of the C=O peak at 1662.5 cm^{-1} decreased and broadened as the MWCNTs content increased in the nanocomposite blend, as indicated in table (3). These findings confirm the interaction between the PVP-PVA blend and the MWCNTs, as reported in reference [24].

The absorption peak at 1439.75 cm^{-1} represents the stretching of the pyridine ring in -C=N, which moves to a higher wavenumber with an increase in the MWCNTs content [18,21]. The peak at 1295 cm^{-1} was assigned to the distinctive band of alkyl (CH in CH_2) groups present in the polymers PVP and PVA [25].

The presence of the band at 1025.5 cm^{-1} provides evidence of the C-O bond. This peak serves as strong confirmation of the successful bonding between PVA and the surface of MWCNTs. It is mostly associated with the crystalline nature of PVA and can be attributed to the stretching of the carboxyl group (C-O) [18]. The peaks at 952 cm^{-1} and 706.5 cm^{-1} correspond to the stretching of C-O and the rocking of CH_2, respectively. These changes in certain characteristic bands can be interpreted as indicators of structural modifications induced by the MWCNTs in the PVP-PVA blend. Alterations in band wavenumbers signify shifts in potential energy distribution along the polymer chain due to the introduction of the filler. Moreover, the double bond segments in the current system have been found to be favorable locations for polarons and/or bipolarons, which could serve as sites for charge carrier hopping [26].

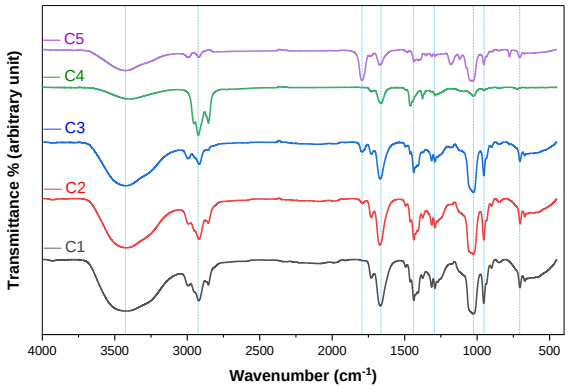

Fig. (2) FTIR spectra of blend nanocomposites with various weight percentages of MWCNTs

The Nyquist plots depict the characteristics of blend nanocomposite electrolytes with varying weight percentages: 2, 4, 6, 8, and 10 wt.% for each nanofiller, namely SiO_2, and MWCNTs are presented in figures (3a and b) and (4a and b), respectively. These plots were obtained at two different temperatures, particularly 293 K and 323 K, which exhibit a distinct spike-like structure at a lower frequency range, while a semicircular pattern is observed at higher frequencies. This semicircular pattern decreases gradually as both temperature and conductivity increase. This behavior can be attributed to the resistive and capacitive properties inherent in the sample [27]. The value of bulk resistance (R_b) was determined by taking the intercept of the semi-circular plot on the real axis. This value was used to calculate the ionic conductivity using Eq. (1) [14]. Introducing nanofillers into the polymer blend resulted in a noticeable reduction in the bulk resistance value and consequently, the resistivity, as evidenced by the observed changes in the Nyquist plot. A decrease in the bulk resistance implies an augmentation in the ionic conductivity [28,29].

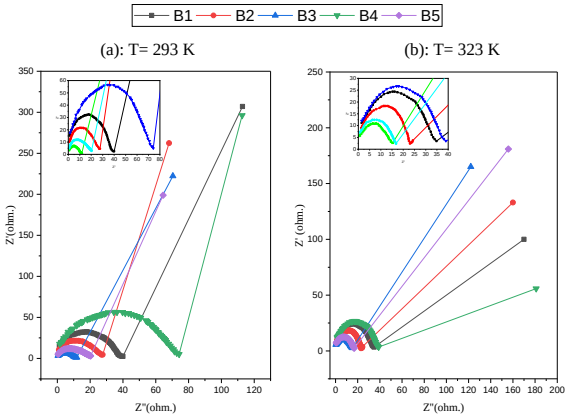

Fig. (3) Nyquist plots for nanocomposite blends containing various weight percentages of SiO_2

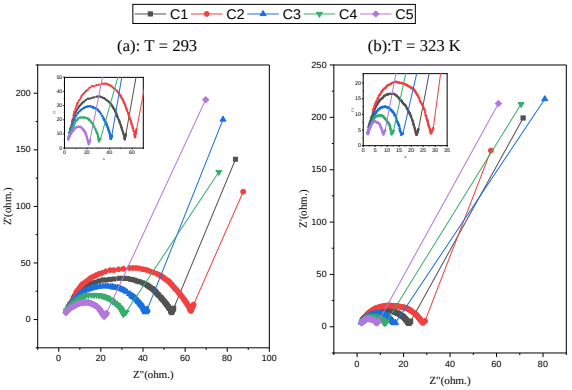

Fig. (4) Nyquist plots for nanocomposite blends containing various weight percentages of MWCNT

The conductivity of the blend electrolytes as a function of temperature and different ratios (2, 4, 6, 8, 10 wt.%) for each nanoparticle (SiO_2 and MWCNTs) over "the temperature range (293-343 K)"illustrated in figures (5a and b). The conductance of gel polymer B and C gradually increases by increasing the temperature, obeying the Arrhenius type thermally activated (ion dynamics associated with thermal activation energy) and expressed as [30]:

$$\sigma = \sigma_{\circ} \exp(\frac{-E_a}{KT}) \qquad (3)$$

where σ is the conductivity, Ea is the activation energy in eV, K is Boltzmann constant and T is the temperature in K [28,29]. Arrhenius-type behavior indicates that ion transport is decoupled from polymer chain respiration via a hopping mechanism. It is evident from the plots that the bulk ionic conductivity

increases as the temperature rises for all nanocomposites electrolytes, in accordance to the findings of previous studies [32].

The charge carrier concentration has a major effect on the conductivity of nanocomposite electrolytes. Hence, it can be predicted that alterations in the concentration of nanofillers will result in associated changes in conductivity. The observed increase in the conductivity can be attributed to the higher concentration of complexation sites present in polymer electrolytes [33], with the rising temperature, the random phase becomes more elastic, resulting in increased part motion of the polymer chains, as represented by enhancing conductance [34].

The observed increase of the conductivity depicted in Fig. (5a) can be attributed to the growth of aggregation as the concentration of nano-SiO_2 increases. As the concentration of SiO_2 increases to 0.06 wt.%, the conductivity increases before declining as seen in Fig. (6a). The electrolyte B3 has the highest conductivity with a value of $9.838x10^{-3}$ S/cm [15].

From Fig. (5b), the highest conductivity of the nanocomposites electrolyte with 10 wt.% of MWCNs (C5) is $1.796x10^{-2}$ (S/cm) at room temperature. The increase in conductivity can be attributed to the increase in number of density and/or mobility of the charge carrier [35]. In Fig. (6b), the conductivity value of the electrolyte C2 decreases, the decrease which may be due to the occurrence of agglomeration and aggregation in some areas within the paths of ions between the polymeric chains, which leads to impeding the movement of ions. This means a decrease in the mobility of ions, and thus a decrease in the conductivity values.

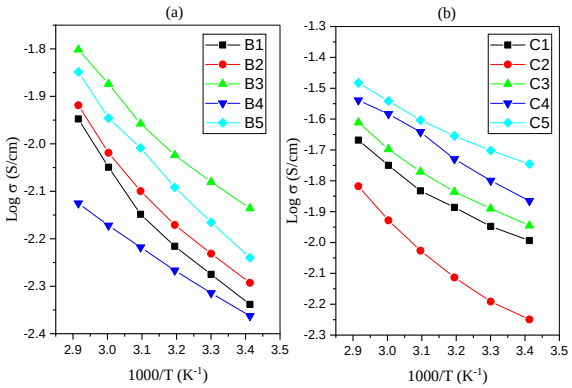

Fig. (5) Ionic conductivity of the electrolytes in blended nanocomposites with (a) SiO_2 and (b) MWCNTs as a function of temperature

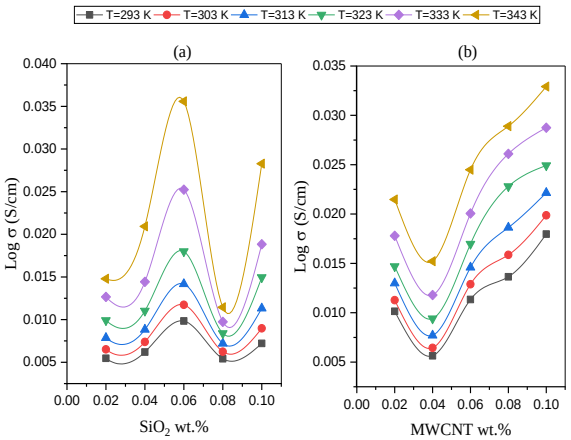

Fig. (6) Ionic conductivity in nanocomposite electrolytes, (a) SiO_2, (b) MWCNTs, is dependent on the weight ratio of the nanofillers

According to Fig. (5), the conductivity increases as the temperature rises, which can be attributed to the great flexible polymer chains. This enhanced flexibility allows for long-distance movement of ions through coordinating sites within the polymer matrix, specifically through the segmental motion of polymer chains [36].

The calculated values of activation energy (Ea) are presented in table (4), demonstrating a decline trend as conductivity increases. The incorporation of nanofillers induces variations in the activity and mobility of carriers, resulting in a reduction in activation energy. It can be reasonably hypothesized that both SiO_2 and MWCNT are uniformly dispersed within the amorphous phase and occupy interstitial positions among the PVP-PVA chains. The introduction of nanofillers in this study establishes a connection with the PVP-PVA chain through the formation of hydrogen bonds. This interaction facilitates the conduction of charges between the nanofillers and the PVP-PVA network [37-39].

Table (4) The conductivity, activation energy, and R^2 regression values at ambient temperature were measured for electrolytes B & C

Electrolytes	σ_{RT} (S/cm)	E_a (eV)	R^2
B1	5.465×10^{-3}	0.0587	0.964
B2	6.198×10^{-3}	0.0473	0.993
B3	9838×10^{-3}	0.0211	0.997
B4	5.413×10^{-3}	0.0656	0.962
B5	7.206×10^{-3}	0.0569	0.979
C1	1.0147×10^{-2}	0.0305	0.976
C2	5.634×10^{-3}	0.0369	0.977
C3	1.1343×10^{-2}	0.0288	0.981
C4	1.3643×10^{-2}	0.0245	0.987
C5	1.7964×10^{-2}	0.0235	0.995

The real dielectric constant (ε_r) was analyzed to further verification in the conductivity trends of the electrolytes. The ε_r signifies the capability of the dielectric material to store charges by conduction [40].

Figure (7) illustrates the relationship between the frequency of blend nanocomposites and the variation of the real dielectric. The findings coincide with the

previous study [41], showing that the real dielectric exhibits higher values in the low-frequency range, but these values decrease as the frequency increases. This phenomenon can be attributed to the behavior of polar materials, which initially possess high real dielectric values. However, as the frequency rises, the value which value? diminishes. This can be explained by the fact that dipoles are unable to respond to rapid changes in the field at higher frequencies, coupled with the presence of polarization effects. At higher frequencies, the electric field undergoes periodic reversals so quickly because of no surplus ion diffusion occurring in the field direction. Consequently, the real dielectric decreases as the frequency increases for all the samples [42]. Furthermore, the dielectric constant (εr) indicates that the rise in the conductivity comes from an increase in the number of free mobile ions or, in simpler terms, as a fractional increase in charge. The increase in available ions is a result of ion dissociation, while the decrease is attributed to ion association [43].

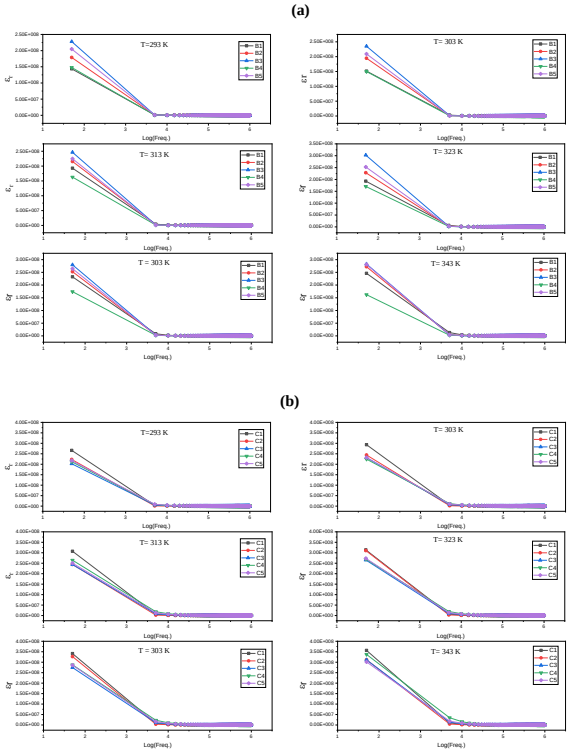

Fig. (7) Dielectric constant as a function ofLog frequency for blend nanocomposites at various temperatures, with various nanoparticles (a): SiO_2, and (b): MWCNTs

Figure (8) displays the DSC thermograms of two types of polymer nanocomposites (PNC) blends, namely (PVP-PVA-SiO_2) and (PVP-PVA-MWCNTs), containing 2 and 10 wt.% of Nanofillers. These DSC curves reveal peaks of endothermic centered at approximately 64.80 ℃ and 99.34 ℃, representing the glass phase transition (T_g) of the PVP-PVA-KI blend with 2 and 10 wt.% of SiO_2, respectively. Similarly, the PVP-PVA-KI blend with equivalent percentages of MWCNTs exhibits T_g values of approximately 67.25°C and 67.95°C, respectively. Table (5) provides the values of T_g, T_m, and ΔH_m of the nanofillers, derived from the DSC curves.

The glass transition temperature (T_g) flexible state arises when the polymer chains experience less constraint on their movement, allowing for greater freedom of motion. This occurs when the interactions between neighboring chains are lost, leading to a significant increase in the local mobility of the polymer backbone. The presence of a single glass transition temperature in the PVP-PVA-KI blend and the polymer blend nanocomposite electrolytes indicates a high level of compatibility between the blended components, particularly in the non-crystalline regions of the polymer blend [44].

Table (5) demonstrates the PNC electrolytes that have lower T_g values than the (PVP-PVA-KI) electrolytes.

The reduction in the T_g in the PNC blend electrolytes, which consist of 2 wt.% SiO_2 and MWCNTs, suggests that the inclusion of dispersed nanoparticles within the PVP-PVA-KI blend structure functions as a plasticizer. The inclusion of nanoparticles within the polymer structure causes a disturbance in the interactions between the PVP and PVA chains, leading to a reduction in the T_g value of the blend in the PNC electrolytes.

The T_m values of nanoparticles containing PVA/PVP/KI blend matrices based PNC electrolytes are higher than the PVA/PVP/KI blend electrolytes (table 1) which confirms the increase in their thermal stability.

The melting temperature (T_m) values of these PNC electrolytes, which depend on the concentration of nanoparticles, demonstrate that incorporating 10 wt.% MWCNTs nanoparticles into the PVP-PVA-KI blend matrix significantly enhances the thermal stability of the polymer blend. The changes observed of the size and shape of the endothermic peak related to T_m are also indicative of the degree of crystallinity and the strength of interactions between the polymer and nanoparticles in the electrolytes [23].

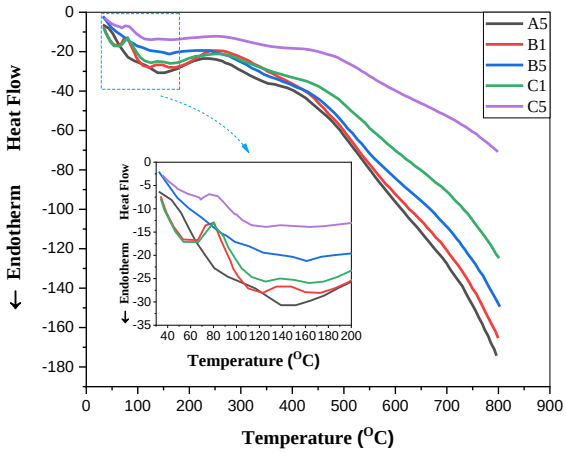

Fig. (2) The DSC thermograms of PNC electrolytes

Table (5) The glass and melting transition phases

Samples	wt.%	T_g (°C)	T_m (°C)	H_m (J/g)	Samples Type
A5	50	141.52	153.21	635.3	KI
B1	2	64.80	143.87	500.7	SiO_2
B5	10	99.34	160.12	425.75	
C1	2	67.25	142.66	205.1	MWCNTs
C5	10	67.95	295.03	287.7	

4. Conclusions

In this study, blend nanocomposite electrolytes based on organic and inorganic nanoparticles were fabricated by solution casting technique. The FTIR analysis of the electrolytes revealed a strong interaction between the polymer blends and the nanoparticles. The presence of nanofillers caused changes in the shape, intensity and position of the stretching modes, indicating their influence on the interactions with the electrolytes. The electrical conductivity was estimated between the frequencies of 50 Hz and 1 MHz and between temperatures of 293 and 343 K. The electrical conductivity change of the nanocomposite electrolytes was found to be dependent on the type and concentration of fillers. At room temperature, the highest conductivity values were observed for the nanocomposite electrolytes 9.838×10^{-3} S/cm and 1.796×10^{-2} S/cm for 6 wt.% of SiO_2 and 10 wt.% of MWCNTs respectively. As the temperature increases, the electrolytes expand which allows a freedom in defects formation and motion that characterized by the Ea. The real dielectric constant (ε_r) increased as the frequency decreased for various weight percentages of nanoparticles. This behavior can be attributed to ion dissociation, leading to an increase in the number of available ions, while ion association causes a decrease. The blend and the nanocomposite electrolytes exhibit a single glass transition temperature which indicate to high level of compatibility between the blend components. The introduction of 10 weight percent of MWCNTs nanoparticles significantly enhanced the thermal stability of the polymer blend matrix.

References

[1] M.A. Abood and B.A. Hasan, "FTIR Analysis and Characterizations of (SnO_2: Ga_2O_3, CeO_2/Cu_2S/c-pSi) Heterojunctions Solar Cells", *Iraqi J. Sci.*, 64(5) (2023) 2282-2296.

[2] D. Ravindran and P. Vickraman, "Influence of Nanomaterials on the Ionic Conductivity and Thermal Properties of Polymer Electrolytes for Li+-Ion Battery Application", *Mater. Sustain. Ener. Stor. Nanoscale*, (2023) 177-191.

[3] W. Wang and P. Alexandridis, "Composite polymer electrolytes: Nanoparticles affect structure and properties", *Polymers*, 8(11) (2016) 387.

[4] X. Chen and X. Kong, "Nanoscale Confinement Effects on Ionic Conductivity of Solid Polymer Electrolytes: The Interplay between Diffusion and Dissociation", *Nano Lett.*, ?? (2023) ??-??.

[5] S. Mousumi, "Nanocomposite Materials", *Nanotechnol. Enviro.*, ?? (2020) ??-??. doi: 10.5772/intechopen.93047.

[6] R.M. Snari et al., "Solution blowing spinning of polylactate/polyvinyl alcohol/ZnO nanocomposite toward green and sustainable preparation of wound dressing nanofibrous films", *Microscopy Res. Tech.*, 85(12) (2022) 3860-3870.

[7] K.R. Aadil et al., "Advanced functional nanomaterials of biopolymers: Structure, properties, and applications", *in Functional Materials from Carbon, Inorganic, and Organic Sources*, Woodhead Publishing (2023) pp. 521-557.

[8] M.-C. Popescu et al., "Structural and morphological evaluation of CNC reinforced PVA/Starch biodegradable films", *Int. J. Biol. Macromol.*, 116 (2018) 385-393.

[9] M. Kurakula and G.S.N. Koteswara Rao, "Pharmaceutical assessment of polyvinylpyrrolidone (PVP): As excipient from conventional to controlled delivery systems with a spotlight on COVID-19 inhibition", *J. Drug Deliv. Sci. Technol.*, 60 (2020) 102046.

[10] D. Puppi and F. Chiellini, "Biodegradable polymers for biomedical additive manufacturing", *Appl. Mater. Today*, 20 (2020) 100700.

[11] A. Kumar, V. Mahto and A. Kumar Choubey, "Synthesis and characterization of cross-linked hydrogels using polyvinyl alcohol and polyvinyl pyrrolidone and their blend for water shut-off treatments", *J. Mol. Liquids*, 301 (2020) 112472.

[12] K. Deshmukh et al., "Fumed SiO_2 nanoparticle reinforced biopolymer blend nanocomposites with high dielectric constant and low dielectric loss for flexible organic electronics", *J. Appl. Polym. Sci.*, 134(5) (2017) ??-??.

[13] L. Lavagna et al., "Functionalization as a way to enhance dispersion of carbon nanotubes in matrices: A review", *Mater. Today Chem.*, 1(20) (2021) 100477.

[14] S.S. Salehan et al., "Conductivity, structural and thermal properties of corn starch-lithium iodide nanocomposite polymer electrolyte incorporated with Al_2O_3", *J. Polym. Res.*, 28(6) (2021) 1-11.

[15] E.A. Swady and M.K. Jawad, "Dependency of the AC conductivity of blend nanocomposites on the Lil and ZnO percent", *in AIP Conf. Proc.*, 2437(1) (2022) 020053.

[16] F.M. Ahmed and S.M. Hassan, "Optical and AC Electrical Properties for Polypyrrole and Polypyrrole/Graphene (ppy/gn) Nanocomposites", *Iraqi J. Phys.*, 19(51) (2021) 72-78.

[17] T. Dippong et al., "A possible formation mechanism and photocatalytic properties of

CoFe2O4/PVA-SiO_2 nanocomposites", *Thermochim. Acta*, 666 (2018) 103-115.
[18] J. Sushma et al., "Investigation of the effect of in-situ grown PPy on low frequency dielectric properties and other properties of PVA-PVP blend film", *J. Adv. Dielect.*, 11(4) (2021) 2150020.
[19] E.M. Abdelrazek and H.M. Ragab, "Spectroscopic and dielectric study of iodine chloride doped PVA/PVP blend, *Indian J. Phys.*, 89(6) (2015) 577-585.
[20] T.S. Soliman, S.A. Vshivkov and S.I. Elkalashy, "Structural, thermal, and linear optical properties of SiO_2 nanoparticles dispersed in polyvinyl alcohol nanocomposite films", *Polym. Comp.*, 41(8) (2020) 3340-3350.
[21] J.O. Dennis et al., "Substantial Proton Ion Conduction in Methylcellulose/Pectin/Ammonium Chloride Based Solid Nanocomposite Polymer Electrolytes: Effect of ZnO Nanofiller", *Membranes*, 12(7) (2022) 706.
[22] M. Ahsani et al., "Preparation and characterization of hydrophilic and antibacterial silver decorated silica-grafted-poly (vinylpyrrolidone)(Ag-SiO_2-PVP) nanoparticles for polymeric nanocomposites", *J. Appl. Polym. Sci.*, 138(38) (2021) 50977.
[23] S. Choudhary, "Characterization of amorphous silica nanofiller effect on the structural, morphological, optical, thermal, dielectric and electrical properties of PVA–PVP blend based polymer nanocomposites for their flexible nanodielectric applications", *J. Mater. Sci.: Mater. in Electron.*, 29(12) (2018) 10517-10534.
[24] M. Irfan et al., "Influence of NaF salt doping on electrical and optical properties of PVA/PVP polymer blend electrolyte films for battery application", *J. Mater. Sci.: Mater. in Electron.*, 32(5) (2021) 5520-5537.
[25] A. El Nemr et al., "Manufacturing of pH sensitive PVA/PVP/MWCNT and PVA/PEG/MWCNT nanocomposites: an approach for significant drug release", *J. Macromol. Sci., Pt. A*, 56(8) (2019) 781-793.
[26] H.M. Zidan et al., "Characterization and some physical studies of PVA/PVP filled with MWCNTs", *J. Mater. Res. Technol.*, 8(1) (2019) 904-913.
[27] P. Singh and A.L. Saroj, "Effect of vibrational, thermal, and ionic conductivity study", *Polym.-Plast. Technol. Mater.*, 60(3) (2021) 298-305.
[28] A.M. Zulkifli et al., "Characteristics of dye-sensitized solar cell assembled from modified chitosan-based gel polymer electrolytes incorporated with potassium iodide", *Molecules*, 25(18) (2020) 4115.
[29] A. Arya, N.G. Saykar and A. Lal Sharma, "Impact of shape (nanofiller vs. nanorod) of TiO_2 nanoparticle on free-standing solid polymeric separator for energy storage/conversion devices", *J. Appl. Polym. Sci.*, 136(16) (2019) 47361.
[30] M.K. Jawad, "Polymer electrolytes based PAN for dye-sensitized solar cells", *Iraqi J. Phys.*, 15(33) (2017) 143-150.
[31] F.M. Ahmed, S.M. Hassan and M.I. Kamil, "The DC electrical conductivity of prepared pure polypyrrole and polypyrrole/graphene (PPY/GN) nanocomposite by *in-situ* polymerization", *Iraqi J. Phys.*, 18(44) (2020) 50-61.
[32] A.S. Mohamed et al., "The development of chitosan-maltodextrin polymer electrolyte with the addition of ionic liquid for electrochemical double layer capacitor (EDLC) application", *Int. J. Electrochem. Sci.*, 17(3) (2022) ??-??.
[33] S.M. Abdalcareem and M.K. Jawad, "Effect of cation size on electrochemical properties of polymer electrolyte", *Iraqi J. Phys.*, 17(42) (2019) 76-84.
[34] A. Abdukarimov et al., "Influence of charge carrier density, mobility and diffusivity on conductivity–temperature dependence in polyethylene oxide–based gel polymer electrolytes", *High Perform. Polym.*, 34(2) (2022) 232-241.
[35] A. Arya and A. Lal Sharma, "Temperature and salt-dependent dielectric properties of blend solid polymer electrolyte complexed with LiBOB", *Macromol. Res.*, 27(4) (2019) 334-345.
[36] S.B. Aziz et al., "A conceptual review on polymer electrolytes and ion transport models", *J. Sci.: Adv. Mater. Dev.*, 3(1) (2018) 1-17.
[37] P. Singh, P.N. Gupta and A.L. Saroj, "Ion dynamics and dielectric relaxation behavior of PVA-PVP-NaI-SiO2 based nano-composites polymer blend electrolytes", *Physica B: Cond. Matter*, 578 (2020) 411850.
[38] H.A.H. Alzahrani, "CuO and MWCNTs nanoparticles Filled PVA–PVP nanocomposites: morphological, optical, thermal, dielectric, and electrical characteristics", *J. Inorg. Organomet. Polym. Mater.*, 32(5) (2022) 1913-1923.
[39] S.S. Salehan et al., "Conductivity, structural and thermal properties of corn starch-lithium iodide nanocomposite polymer electrolyte incorporated with Al_2O_3", *J. Polym. Res.*, 28(6) (2021) 1-11.
[40] M.A. Morsi, A. Rajeh and A.A. Al-Muntaser, "Reinforcement of the optical, thermal and electrical properties of PEO based on MWCNTs/Au hybrid fillers: nanodielectric materials for organoelectronic devices", *Composites Pt. B: Eng.*, 173 (2019) 106957.
[41] B.A. Hasan and H.H. Issa, "Dielectric properties and AC electrical conductivity analysis of $(La_2O_3)_{1-x}(ZnO)_x$", *in IOP Conf. Ser.: Mater. Sci. Eng.*, 928(7) (2020) 072003.
[42] M. Irfan et al., "Influence of NaF salt doping on electrical and optical properties of PVA/PVP

polymer blend electrolyte films for battery application", *J. Mater. Sci.: Mater. in Electron.*, 32(5) (2021) 5520-5537.

[43] F.M. Ahmed and M.K. Jawad, "FTIR and electrical behavior of blend electrolytes based on (PVA/PVP)", *Iraqi J. Phys.*, 21(1) (2023) 1-9.

[44] M.T. Ramesan et al., "Influence of copper sulphide nanoparticles on the structural, mechanical and dielectric properties of poly (vinyl alcohol)/poly (vinyl pyrrolidone) blend nanocomposites", *J. Mater. Sci.: Mater. in Electron.*, 29 (2018) 1992-2000.

Table (2) the band of blend nanocomposites with SiO_2

The wavenumber (cm^{-1}) of a blend comprising of pure PVP-PVA-KI with varying concentrations of SiO_2 weight percentage.					Assignments
2 %	4%	6%	8%	10%	
3414.78	3441.75	3415.75	3417	3428.38	**Si-OH Stretching/vibration**
2990.59		2982.25	2988.75		**C-H stretching**
2926.75	2920.75	2911.75	2912	2924	**C-H asymmetric stretching vibration**
2825.22		2830	2821	2853.5	**C-H symmetric stretching**
1793.49	1798.5	1794.25	1800.5	1800.88	**C=O stretching**
1665.25	1673.25	1672.75	1675.5	1674.88	**-C=O stretching**
1437.72	1437.75	1439.25	1436.25	1434.25	**-C=N pyridine ring/stretching**
1289.96	1179.25	1183.75	1182	1179.88	**CH_2 twisting**
1036.67			1052.75	1049.75	**Si-O-Si asymmetric stretching vibration**
953.85	955	952.5	957.25	956.38	**Si-O-Si asymmetric stretching vibration**
	776.75	775.5	776.5	776.75	**Si-O-Si asymmetric stretching vibration**
703.69	709.5	713.75	704.25	713.88	**Si-O-Si symmetric stretching vibration**

Table (3) The band of blend nanocomposites with MWCNs

The wave number (cm^{-1}) of a blend comprising pure PVP-PVA-KI with varying concentrations of MWCNTs weight percent.					Assignments
2 %	4%	6%	8%	10%	
3426.5	3118.5	3424.5	3402	3419.32	OH stretching
2925.5	2919.25	2917.75	2853.5	2919.9	CH_2 asymmetric stretching deriving from PVA
	1794.5	1793.75		1794.5	C=C stretching
1662.5	1675.75	1668.5	1664	1666.98	C=O stretching deriving from PVP
1439.75	1433.25	1438.5	1461	1436.43	-C=N pyridine ring/stretching
1295	1291.25	1290			C-H wagging deriving from PVA
1025.5	1018.5	1028.75	1025.25	1033.15	C-O stretching
952	953.25	953.5	952.75	952.25	C-O stretching vibrations deriving from PVA
706.5	703.25	705.25	720.75	703.5	CH_2 wagging

